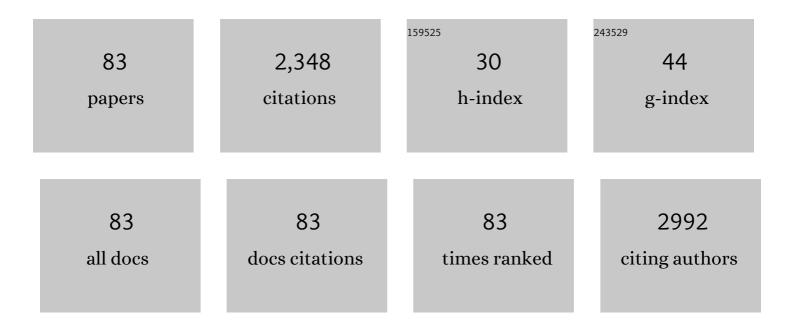
List of Publications by Year in descending order

Source: https://exaly.com/author-pdf/3159853/publications.pdf Version: 2024-02-01



#	Article	IF	CITATIONS
1	Microwave-triggered ionic liquid-based hydrogel dressing with excellent hyperthermia and transdermal drug delivery performance. Chemical Engineering Journal, 2022, 429, 131590.	6.6	28
2	A turn-on fluorescent probe via substitution-rearrangement for highly sensitive and discriminative detection of cysteine and its imaging in living cells. Spectrochimica Acta - Part A: Molecular and Biomolecular Spectroscopy, 2022, 266, 120409.	2.0	13
3	Aptamer/AuNPs encoders endow precise identification and discrimination of lipoprotein subclasses. Biosensors and Bioelectronics, 2022, 196, 113743.	5.3	6
4	Fabrication and application of 2,4,6-trinitrophenol sensors based on fluorescent functional materials. Journal of Hazardous Materials, 2022, 425, 127987.	6.5	32
5	Metal–Organic Frameworks Encapsulating Carbon Dots Enable Fast Speciation of Mono- and Divalent Copper. Analytical Chemistry, 2022, 94, 2255-2262.	3.2	9
6	lonic liquids enable the preparation of a copper-loaded gel with transdermal delivery function for wound dressings. Biomaterials Science, 2022, 10, 1041-1052.	2.6	12
7	Aptamer-Based Cell Nucleus Imaging via Expansion Microscopy. Analytical Chemistry, 2022, 94, 6044-6049.	3.2	7
8	Tailoring the Phase Transition and Luminescence Behaviors of a Poly(ionic liquid) to Ensure Visual Temperature Sensing. ACS Applied Polymer Materials, 2022, 4, 191-199.	2.0	4
9	Modulation of the binding ability to biomacromolecule, cytotoxicity and cellular imaging property for ionic liquid mediated carbon dots. Colloids and Surfaces B: Biointerfaces, 2022, 216, 112552.	2.5	4
10	Kadsura-Shaped Covalent–Organic Framework Nanostructures for the Sensitive Detection and Removal of 2,4,6-Trinitrophenol. ACS Applied Nano Materials, 2022, 5, 6422-6429.	2.4	19
11	The concurrent enrichment of glycoproteins and phosphoproteins with polyoxometalate-covalent organic framework conjugate as the adsorbent. Journal of Chromatography A, 2022, 1675, 463183.	1.8	2
12	State-of-the-art advances of copper-based nanostructures in the enhancement of chemodynamic therapy. Journal of Materials Chemistry B, 2021, 9, 250-266.	2.9	92
13	Precise regulation of the properties of hydrophobic carbon dots by manipulating the structural features of precursor ionic liquids. Biomaterials Science, 2021, 9, 3127-3135.	2.6	4
14	A Salt Stimulus-Responsive Nanohydrogel for Controlled Fishing Low-Density Lipoprotein with Superior Adsorption Capacity. ACS Applied Materials & Interfaces, 2021, 13, 4583-4592.	4.0	14
15	Ionic liquid modification of metal-organic framework endows high selectivity for phosphoproteins adsorption. Analytica Chimica Acta, 2021, 1147, 144-154.	2.6	11
16	Research progress of ionic liquids-based gels in energy storage, sensors and antibacterial. Green Chemical Engineering, 2021, 2, 368-383.	3.3	27
17	"Switch-on―fluorescence sensing platform based on porphyrin metal-organic frameworks for rapid and specific detection of zinc ion. Analytical and Bioanalytical Chemistry, 2021, 413, 5161-5168.	1.9	8
18	Construction of Novel Nanocomposites (Cu-MOF/GOD@HA) for Chemodynamic Therapy. Nanomaterials, 2021, 11, 1843.	1.9	24

#	Article	IF	CITATIONS
19	Mutual Benefit between Cu(II) and Polydopamine for Improving Photothermal–Chemodynamic Therapy. ACS Applied Materials & Interfaces, 2021, 13, 38127-38137.	4.0	56
20	β-Naphthothiazolium-based ratiometric fluorescent probe with ideal pKa for pH imaging in mitochondria of living cells. Talanta, 2021, 232, 122475.	2.9	17
21	Upconversion nanoparticles/carbon dots (UCNPs@CDs) composite for simultaneous detection and speciation of divalent and trivalent iron ions. Analytica Chimica Acta, 2021, 1183, 338973.	2.6	6
22	Effects of alkyl side-chain length on binding with bovine serum albumin, cytotoxicity, and antibacterial properties of 1-alkyl-3-methylimidazolium dicyanamide ionic liquids. Journal of Molecular Liquids, 2021, 339, 116835.	2.3	4
23	The anion of choline-based ionic liquids tailored interactions between ionic liquids and bovine serum albumin, MCF-7 cells, and bacteria. Colloids and Surfaces B: Biointerfaces, 2021, 206, 111971.	2.5	16
24	Imaging vicinal dithiol of arsenic-binding proteins in the mouse brain with amplification by gold nanocluster Au22(GSH)18. Chemical Communications, 2021, 57, 3103-3106.	2.2	4
25	Functionalized polyoxometalate microspheres ensure selective adsorption of phosphoproteins and glycoproteins. Chemical Communications, 2021, 57, 3367-3370.	2.2	13
26	Mitochondria-targeted ratiometric fluorescent imaging of cysteine. Analyst, The, 2021, 146, 4642-4648.	1.7	7
27	Chondroitin sulfate-enriched hierarchical multichannel polydopamine nanoparticles with ultrahigh sorption capacity for separation of low-density lipoprotein. Journal of Materials Chemistry B, 2021, 9, 1980-1987.	2.9	3
28	Simultaneous metabolomics and proteomics analysis of plasma-derived extracellular vesicles. Analytical Methods, 2021, 13, 1930-1938.	1.3	18
29	Sensitivity Dependence on the Crystal Forms of a Fluorescence Quencher for Silicon Quantum Dots and Its Use in Acetylcholinesterase Assay. Analytical Chemistry, 2021, 93, 14900-14906.	3.2	10
30	Membrane-Activated Fluorescent Probe for High-Fidelity Imaging of Mitochondrial Membrane Potential. ACS Sensors, 2021, 6, 4009-4018.	4.0	23
31	Ultrasmall Copper–Gallic Acid Nanodots for Chemodynamic Therapy. Advanced Materials Interfaces, 2021, 8, 2101173.	1.9	14
32	Chondroitin sulfate-functionalized 3D hierarchical flower-type mesoporous silica with a superior capacity for selective isolation of low density lipoprotein. Analytica Chimica Acta, 2020, 1104, 78-86.	2.6	8
33	Boronic acid modified polyoxometalate-alginate hybrid for the isolation of glycoproteins at neutral environment. Talanta, 2020, 210, 120620.	2.9	16
34	A fluorescence imaging protocol for correlating intracellular free cationic copper to the total uptaken copper by live cells. Talanta, 2020, 220, 121355.	2.9	11
35	Simultaneous detection and speciation of mono- and di-valent copper ions with a dual-channel fluorescent nanoprobe. Chemical Communications, 2020, 56, 15337-15340.	2.2	10
36	Copper-Cysteamine Nanoparticles as a Heterogeneous Fenton-Like Catalyst for Highly Selective Cancer Treatment. ACS Applied Bio Materials, 2020, 3, 1804-1814.	2.3	69

#	Article	IF	CITATIONS
37	Poly(ionic liquid)-Gated CuCo ₂ S ₄ for pH-/Thermo-Triggered Drug Release and Photoacoustic Imaging. ACS Applied Materials & Interfaces, 2020, 12, 9000-9007.	4.0	23
38	Europium–Pyridinedicarboxylate–Adenine Light-Up Fluorescence Nanoprobes for Selective Detection of Phosphate in Biological Fluids. ACS Applied Materials & Interfaces, 2020, 12, 22593-22600.	4.0	45
39	Improvement of antibacterial activity of copper nanoclusters for selective inhibition on the growth of gram-positive bacteria. Chinese Chemical Letters, 2019, 30, 421-424.	4.8	42
40	Glutathione triggered degradation of polydopamine to facilitate controlled drug release for synergic combinational cancer treatment. Journal of Materials Chemistry B, 2019, 7, 6742-6750.	2.9	49
41	In situ fabrication of organic electrochemical transistors on a microfluidic chip. Nano Research, 2019, 12, 1943-1951.	5.8	16
42	The structure-activity relationship of hydrophilic carbon dots regulated by the nature of precursor ionic liquids. Journal of Colloid and Interface Science, 2019, 554, 722-730.	5.0	13
43	Ionic liquid mediated carbon dots: Preparations, properties and applications. TrAC - Trends in Analytical Chemistry, 2019, 119, 115638.	5.8	31
44	Intracellular Zinc Quantification by Fluorescence Imaging with a FRET System. Analytical Chemistry, 2019, 91, 4157-4163.	3.2	33
45	Gold Nanoclusters/Iron Oxyhydroxide Platform for Ultrasensitive Detection of Butyrylcholinesterase. Analytical Chemistry, 2019, 91, 15866-15872.	3.2	33
46	AC Electrodeposition of PEDOT Films in Protic Ionic Liquids for Long-Term Stable Organic Electrochemical Transistors. Molecules, 2019, 24, 4105.	1.7	5
47	A facile method for the synthesis of copper–cysteamine nanoparticles and study of ROS production for cancer treatment. Journal of Materials Chemistry B, 2019, 7, 6630-6642.	2.9	57
48	Improvement on the extraction efficiency of low density lipoprotein in an ionic liquid microemulsion. Talanta, 2019, 195, 720-727.	2.9	12
49	β yclodextrinâ€Decorated Carbon Dots Serve as Nanocarriers for Targeted Drug Delivery and Controlled Release. ChemNanoMat, 2019, 5, 479-487.	1.5	32
50	Folic acid modified copper nanoclusters for fluorescent imaging of cancer cells with over-expressed folate receptor. Mikrochimica Acta, 2018, 185, 205.	2.5	30
51	Thermo/pH dual-stimuli-responsive drug delivery for chemo-/photothermal therapy monitored by cell imaging. Talanta, 2018, 181, 278-285.	2.9	55
52	Functionalization of mesoporous organosilica nanocarrier for pH/glutathione dual-responsive drug delivery and imaging of cancer therapy process. Talanta, 2018, 177, 203-211.	2.9	22
53	Detection of yeast Saccharomyces cerevisiae with ionic liquid mediated carbon dots. Talanta, 2018, 178, 818-824.	2.9	9
54	Core–Corona Magnetic Nanospheres Functionalized with Zwitterionic Polymer Ionic Liquid for Highly Selective Isolation of Glycoprotein. Biomacromolecules, 2018, 19, 53-61.	2.6	38

#	Article	IF	CITATIONS
55	Ionic liquid-based slab optical waveguide sensor for the detection of ammonia in human breath. Journal of Colloid and Interface Science, 2018, 512, 819-825.	5.0	42
56	Probing pH variation in living cells and assaying hemoglobin in blood with nitrogen enriched carbon dots. Talanta, 2018, 188, 788-794.	2.9	15
57	Complexes of magnetic nanospheres with amphiprotic polymer–Zn systems for the selective isolation of lactoferrin. Journal of Materials Chemistry B, 2018, 6, 5596-5603.	2.9	8
58	Protein-Stabilized Gadolinium Oxide-Gold Nanoclusters Hybrid for Multimodal Imaging and Drug Delivery. ACS Applied Materials & Interfaces, 2017, 9, 6941-6949.	4.0	73
59	A magnetic polypyrrole/iron oxide core/gold shell nanocomposite for multimodal imaging and photothermal cancer therapy. Talanta, 2017, 171, 32-38.	2.9	47
60	Ionic liquid mediated organophilic carbon dots for drug delivery and bioimaging. Carbon, 2017, 114, 324-333.	5.4	97
61	Hollow Copper Sulfide Nanosphere–Doxorubicin/Graphene Oxide Core–Shell Nanocomposite for Photothermo-chemotherapy. ACS Biomaterials Science and Engineering, 2017, 3, 3230-3235.	2.6	41
62	Aptamer-anchored di-polymer shell-capped mesoporous carbon as a drug carrier for bi-trigger targeted drug delivery. Journal of Materials Chemistry B, 2017, 5, 6882-6889.	2.9	25
63	Mesoporous carbon nanoparticles capped with polyacrylic acid as drug carrier for bi-trigger continuous drug release. Journal of Materials Chemistry B, 2016, 4, 5178-5184.	2.9	36
64	Improving the biocompatibility of carbon nanodots for cell imaging. Talanta, 2016, 161, 54-61.	2.9	15
65	Glutathione-mediated mesoporous carbon as a drug delivery nanocarrier with carbon dots as a cap and fluorescent tracer. Nanotechnology, 2016, 27, 355102.	1.3	29
66	Magnetic Nanospheres Encapsulated by Mesoporous Copper Oxide Shell for Selective Isolation of Hemoglobin. ACS Applied Materials & Interfaces, 2016, 8, 29734-29741.	4.0	34
67	Hydrophobic Carbon Nanodots with Rapid Cell Penetrability and Tunable Photoluminescence Behavior for in Vitro and in Vivo Imaging. Langmuir, 2016, 32, 12221-12229.	1.6	45
68	Glutathione functionalized mesoporous organosilica conjugate for drug delivery. RSC Advances, 2016, 6, 56287-56293.	1.7	4
69	Enantiomeric separation of citalopram analogues by HPLC using macrocyclic glycopeptide and cyclodextrin based chiral stationary phases. Journal of Liquid Chromatography and Related Technologies, 2016, 39, 154-160.	0.5	13
70	Separation of curcuminoids using ionic liquid based aqueous two-phase system coupled with in situ dispersive liquid–liquid microextraction. Talanta, 2016, 149, 6-12.	2.9	40
71	Protein-modified hollow copper sulfide nanoparticles carrying indocyanine green for photothermal and photodynamic therapy. Journal of Materials Chemistry B, 2016, 4, 105-112.	2.9	82
72	Enantiomeric Separations of Ruthenium (II) Polypyridyl Complexes Using HPLC With Cyclofructan Chiral Stationary Phases. Chirality, 2015, 27, 64-70.	1.3	27

#	Article	IF	CITATIONS
73	Separation of therapeutic peptides with cyclofructan and glycopeptide based columns in hydrophilic interaction liquid chromatography. Journal of Chromatography A, 2015, 1390, 50-61.	1.8	15
74	The regulation of hydrophilicity and hydrophobicity of carbon dots via a one-pot approach. Journal of Materials Chemistry B, 2015, 3, 6013-6018.	2.9	36
75	Ionic liquid poly(3-n-dodecyl-1-vinylimidazolium) bromide as an adsorbent for the sorption of hemoglobin. RSC Advances, 2015, 5, 31496-31501.	1.7	19
76	A dual-ionic liquid microemulsion system for the selective isolation of hemoglobin. RSC Advances, 2014, 4, 8177.	1.7	29
77	Novel polymeric ionic liquid microspheres with high exchange capacity for fast extraction of plasmid DNA. Analytica Chimica Acta, 2014, 837, 64-69.	2.6	39
78	Fluorescence Enhancement of Imidazolium Ionic Liquid by Its Confinement on PVC for In Situ Selective Quantification of Hemoglobin. ACS Applied Materials & Interfaces, 2013, 5, 12156-12162.	4.0	24
79	Encapsulation of silica nano-spheres with polymerized ionic liquid for selective isolation of acidic proteins. Analytical and Bioanalytical Chemistry, 2013, 405, 8799-8806.	1.9	25
80	New Insight into Molecular Interactions of Imidazolium Ionic Liquids with Bovine Serum Albumin. Journal of Physical Chemistry B, 2011, 115, 12306-12314.	1.2	221
81	Ionic liquid–polyvinyl chloride ionomer for highly selective isolation of basic proteins. Talanta, 2010, 81, 637-642.	2.9	60
82	A reverse microemulsion of water/AOT/1-butyl-3-methylimidazolium hexafluorophosphate for selective extraction of hemoglobin. Separation and Purification Technology, 2008, 64, 154-159.	3.9	41
83	Plasmon Resonance-Inspired Discriminator Unscrambles Lipoprotein Subtypes. Analyst, The, 0, , .	1.7	0